Anal Bioanal Chem
DOI 10.1007/s00216-016-9554-4

RESEARCH PAPER

Carbon dots-decorated multiwalled carbon nanotubes nanocomposites as a high-performance electrochemical sensor for detection of H_2O_2 in living cells

Jing Bai[1] · **Chunhe Sun**[1] · **Xiue Jiang**[1]

Received: 19 January 2016 / Revised: 30 March 2016 / Accepted: 7 April 2016

Abstract A novel enzyme-free hydrogen peroxide sensor composed of carbon dots (CDs) and multi-walled carbon nanotubes (MWCNTs) was prepared. It was found that the carbon dots-decorated multi-walled carbon nanotubes nanocomposites (CDs/MWCNTs) modified glassy carbon (GC) electrode (CDs/MWCNTs/GCE) exhibited a significant synergistic electrocatalytic activity towards hydrogen peroxide reduction as compared to carbon dots or multi-walled carbon nanotubes alone, and the CDs/MWCNTs/GCE has shown a low detection limit as well as excellent stability, selectivity, and reproducibility. These remarkable analytical advantages enable the practical application of CDs/MWCNTs/GCE for the real-time tracking of hydrogen peroxide (H_2O_2) released from human cervical cancer cells with satisfactory results. The enhanced electrochemical activity can be assigned to the edge plane-like defective sites and lattice oxygen in the CDs/MWCNTs nanocomposites due to the small amount of decoration of carbon dots on the multi-walled carbon nanotubes. Based on a facile preparation method and with good electrochemical properties, the CDs/MWCNTs nanocomposites represent a new class of carbon electrode for electrochemical sensor applications.

Keywords Carbon quantum dots · Catalyst · Extracellular H_2O_2 · Electrocatalysis · Nonenzymatic biosensor

Introduction

Hydrogen peroxide (H_2O_2), as an important chemical, is an essential intermediate in food [1], pharmaceutical [2], clinical [3], and environmental analysis [4] and is also a signaling molecule associated with severe human diseases such as cancers, progressive neurodegenerative diseases, Parkinson's disease, etc. [5, 6]. Therefore, accurate and sensitive determination of H_2O_2 has been a challenging requirement in recent years. So far, many methods have been developed for detection of H_2O_2 concentration, including titrimetry [7], chromatography [8], spectrophotometry [9], and electrochemical method [10]. Among them, the electrochemical method has received more attention due to its high sensitivity, low cost, convenient operation, and fast response [11, 12]. Until now, most studies on this subject have focused on enzyme-based sensor [13–15]. Unfortunately, due to the intrinsic nature of enzymes, the enzyme-based biosensors inevitably suffer from environmentally instability, high cost, and complicated immobilization procedure [16–18]. Therefore, development of novel electrocatalyst that can overcome the disadvantages of native enzymes has been desired.

To address this important issue, considerable effort has been put to develop various electrode materials as alternatives to enzymes, such as metal nanoparticles (Au, Pt, Ag, Cu, Rh, and Pd) [19, 20], metal oxides (CuO, Fe_3O_4, TiO_2, and CeO_2) [21, 22], and carbon-based nanomaterials (graphene, carbon nanotubes, carbon nanofibers, and carbon quantum dots) [23, 24]. Among various reports, carbon-based nanomaterials have attracted much physical, chemical, and material research interests because of their high electrical conductivity, large

Electronic supplementary material The online version of this article (doi:10.1007/s00216-016-9554-4) contains supplementary material, which is available to authorized users.

✉ Xiue Jiang
jiangxiue@ciac.ac.cn

[1] State Key Lab of Electroanalytical Chemistry, Changchun Institute of Applied Chemistry, Chinese Academy of Sciences, Changchun, Jilin 130022, China

Published online: 23 April 2016

surface area, high thermal and mechanical stability, and low-cost production. Carbon materials are not only used as support but also as highly active catalysts. The outstanding electrocatalytic activities depend on the presence of certain metal heterocyclic molecules [25] or defective sites onto the carbon material surface [26, 27], but pure activated carbon itself is chemical inertness and commonly exhibits low catalytic activity [28]. An efficient method to improve electrocatalytic activity of carbon material is to introduce heteroatoms and abundant defects onto carbon frameworks to increase the number of catalytic sites. For example, Zhou and co-workers had constructed a OMC-C_{60} system to facilitate heterogeneous electron-transfer processes by increasing edge plane-like defective sites (EDSs) of ordered mesoporous carbon [26]. The OMC-C_{60} system showed a promising electrocatalysis for some important biomolecules. Gong et al. reported that nitrogen-doped carbon nanotube (NCNTs) can act as a metal-free catalyst with a much better electrocatalytic activity, long-term operation stability, and tolerance to crossover effect than platinum for oxygen reduction in alkaline fuel cells [29]. Shao et al. reported that *N*-graphene exhibited much higher electrocatalytic activity towards oxygen and H_2O_2 reduction than graphene and expensive Pt [30]. The results indicate that the presence of edge plane-like defective sites on nanostructured carbon materials improves the electrocatalytic activity of materials.

Carbon dots (CDs), as a zero-dimensional carbon, have received considerable interest due to their outstanding electronic, optical, electrochemical properties [5, 31, 32]. Especially, the emission from carbon dots could be efficiently quenched by either electron acceptor or donor molecules in solution, indicating that the photo-excited carbon dots are excellent as both electron donors and electron acceptors. Therefore, unlike the common carbon material, carbon dot with small size, provide high electrocatalytic activity owing to the large surface area [33–35], but they lower electron transport efficiency owing to the oxygen-rich functional groups, abundant grain boundaries, and defects [36]. This suggests the single carbon dots as the electrode material is not a good choice. Therefore, exploring low-cost and sustainable electrode materials with high conductivity and superior electrocatalytic activity is critical for the development of sensors.

To combine both high electrical conductivity and superior electrocatalytic activity in one material, we reported on the use of carbon dots-decorated multi-walled carbon nanotubes (CDs/MWCNTs) system as an effective sensing platform. In this system, MWCNTs as electron acceptor are selected as matrix material due to its good electrical conductivity and large surface, and CDs as excellent electron donor are used as doped catalyst. The obtained nanocomposites containing CDs and MWCNTs can simultaneously provide high electrical conductivity and superior electrocatalytic activity. The hydrogen peroxide was employed as the probe molecules to study the electrocatalytic behavior of CDs/MWCNTs nanocomposites for the first time. The CDs/MWCNTs nanocomposites show synergistic enhancement electrochemical performance towards hydrogen peroxide reduction compared with CDs or MWCNTs alone. Our research opens up a new opportunity on carbon-based nanomaterials for biosensor.

Experimental

Materials and apparatus

Multi-walled carbon nanotubes were purchased from Shenzhen Nanotech. Port. (Shenzhen, China). Catechol, $NH_3{\cdot}H_2O$ and H_2O_2 (30 wt%) were purchased from Aladin Ltd. (Shanghai, China). The 0.1 M pH 7.4 phosphate buffer solution (PBS) was prepared by mixing 19 mL of 0.1 M NaH_2PO_4 and 81 mL of 0.1 M $Na_2HPO_4{\cdot}7H_2O$ and was employed as a supporting electrolyte in the electrochemical experiment. Catalase was purchased from Sigma-Aldrich. Dulbecco's modified eagle medium (DMEM), penicillin, fetal bovine serum (FBS), and streptomycin were purchased from Beijing Dingguo Biotechnology Co. The human serum samples were taken from volunteers. All chemicals were used as received without further purification. All solutions were freshly prepared with deionized water.

Transmission electron microscopy (TEM) images were obtained from HITACHI H-8100EM (Hitachi, Tokyo, Japan). Raman spectra were obtained on a J-Y T64000 Raman spectrometer with a 514.5-nm wavelength incident laser light. X-ray photoelectron spectroscopy (XPS) analysis was carried on an ESCALAB 250 X-ray photoelectron spectrometer with a monochromated X-ray source (Al Kα hν = 1486.6 eV). All the electrochemical experiments were performed with a CHI830C electrochemical workstation (Shanghai Chenhua Instrument Corporation, China) in a conventional three-electrode cell at room temperature. All solutions were purged with high-purity nitrogen for at least 30 min to remove oxygen prior to the experiments.

Synthesis of carbon dots

In a typical synthesis of CDs, ammonia aqueous solution (2 mL, $NH_3{\cdot}H_2O$, 30 %) was mixed with ethanol (30 mL) under mild stirring at 30 °C for 30 min. Catechol (0.1 g) was added into the above mixture solution. The reaction was continued for 24 h. The color of this solution gradually changed to dark brown. A CDs solution of 1.5 mg/mL was stocked for the further use.

Preparation of CDs/MWCNTs nanocomposites

Before the experiment, the pristine MWCNTs were stirred in HCl and HNO_3 (v/v = 3:1) mixed solution for 30 min at room temperature to remove residual metal catalysts. The treated MWCNTs were rinsed with deionized water until the pH of solution reached to 7.0. Finally, the purified MWCNTs (1.0 mg/mL) were dispersed well in water. Three kinds of CDs/MWCNTs nanocomposites were prepared by mixing different radio of MWCNTs to CDs with sonication and stirring. Briefly, 5 mL of MWCNTs solution (1.0 mg/mL) was mixed with 2, 1, and 0.5 mL of CDs solution (0.5 mg/mL). The mixture was ultrasound for 1 h and stirred for overnight. Then, the mixture was centrifuged at 12,000 rpm for 10 min and washed with water. Finally, the CDs/MWCNTs nanocomposites (5.0 mg/mL) were dispersed well in water for modified electrode. The final products were named as CDs/MWCNTs-5, CDs/MWCNTs-10, and CDs/MWCNTs-20 respectively.

Electrode preparation

Prior to the modification, the glassy carbon electrode (GCE) was polished with 1.0, 0.3, and 0.05 μm alumina slurry, respectively, and sonicated successively in 1:1 nitric acid, absolute alcohol, and double-distilled water. The cleaned electrode was dried with high-purity nitrogen steam. CDs/MWCNTs nanocomposites modified GCE (CDs/MWCNTs/GCE) was prepared by casting 5 μL of CDs/MWCNTs suspension on GCE surface and the solvent evaporated under an infrared lamp. For comparison, CDs modified GCE (CDs/GCE) and MWCNTs modified GCE (MWCNTs/GCE) were prepared in the same way.

Results and discussion

Characterization of CDs/MWCNTs nanocomposites

CDs were firstly prepared by the hydrothermal treatment of catechol at 30 °C in ethanol solution. The TEM was used to record the morphologies of the nanomaterials, as shown in Fig. 1 and Electronic Supplementary Material (ESM) Fig. S1. It can be seen that the CDs are spherical in morphology, and they are separated from each other, indicating that the CDs are well dispersed in water (Fig. 1a). The histograms of the particle size distribution reveals that the average diameter of the CDs is 6.5 nm, as determined by statistical analysis of more than 100 particles (see ESM Fig. S2). To characterize the synthesized CDs, the UV–vis absorption spectra of the aqueous dispersion of the CDs were shown in ESM Fig. S3a. Comparable to precursor catechol, a typical UV–vis absorption at 330 nm corresponding to the n–π* transition of C═O was observed, which is similar to those of previous reports on CDs [37]. The photograph of the dispersion under UV light (365 nm) exhibits a green color, further revealing that the resultant CDs exhibit green fluorescence (see ESM inset of Fig. S3a). To further explore their optical properties, the photoluminescence spectroscopy (PL) of the CDs was studied using different excitation wavelengths. A wavelength excitation dependence of normalized integrated PL intensity was shown in ESM Fig. S3b. It was observed that the emission peak of the CDs shifts from 430 to 580 nm and the intensity decrease gradually with a dependence on the excitation wavelengths from 360 to 420 nm (see ESM inset of Fig. S3b), suggesting the formation of CDs.

Figure 1b shows the as-received MWCNTs where the tubular structure of nanotubes is observed. The diameter of MWCNTs is about 35 nm, and the length is about a few micrometers. By mixing CDs solution with MWCNTs, a large number of CDs were well supported on MWCNTs with negligible nanoparticle aggregation, forming the CDs/MWCNTs-10 nanocomposites, as shown in Fig. 1c. No free nanoparticles were observed outside the MWCNTs, which further confirmed that the CDs/MWCNTs-10 nanocomposites were synthesized successfully.

Electrochemical characterization of the modified electrodes

The cyclic voltammetric behaviors of different modified electrodes were studied using 5.0 mM $[Fe(CN)_6]^{3-/4-}$ as an electrochemical probe in PBS, pH 7.0 containing 0.1 M KCl as shown in Fig. 2a. All electrodes show obvious redox peak. The peak-to-peak separations (ΔE_p) are 120, 194, 92, and 75 mV for bare GCE, CDs/GCE, MWCNTs/GCE, and CDs/MWCNTs-10/GCE, respectively. Also, the CDs/MWCNTs-10/GCE leads to the largest peak current among all kinds of electrodes. These results suggest that the CDs/MWCNTs-10/GCE exhibits faster electron-transfer kinetics and larger electroactive surface area compared to other electrodes. The capability of electron transfer of modified electrodes was further investigated by electrochemical impedance spectroscopy (EIS). Figure 2b shows the Nysquist plots of different electrodes in 5.0 mM $[Fe(CN_6]^{3-/4-}$ solution. R_{ct} denotes the charge transfer resistance of the redox marker between the solution and the electrode surface. By fitting the data (inset of Fig. 2b), it can be seen that the sequence of R_{ct} can be estimated to be CDs/GCE > bare GCE > MWCNTs/GCE > CDs/MWCNTs-10/GCE. This result is in agreement with above cyclic voltammetry results where CDs/MWCNTs-10 nanocomposites were found to have a fast heterogeneous electron transfer rate. The results demonstrate that the CDs/MWCNTs-10/GCE has higher electrochemical activity than CDs/GCE and MWCNTs/GCE. The improvement could be attributed to a synergetic effect of CDs and MWCNTs in this hybrid material.

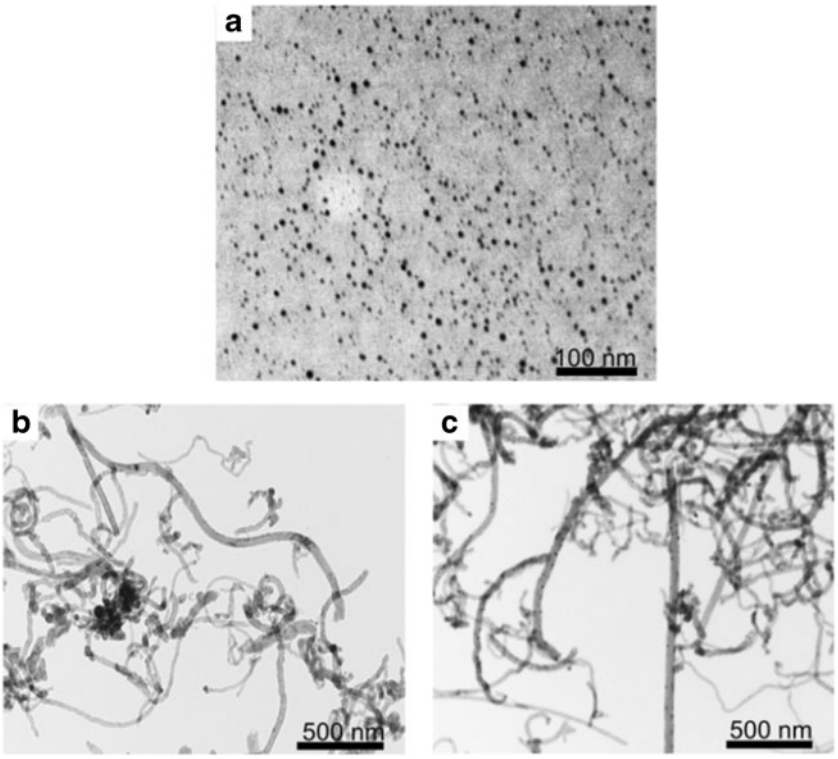

Fig. 1 TEM images of **a** CDs, **b** MWCNTs, and **c** CDs/MWCNTs-10

Electrochemical measurement

To gain insight into the electrocatalytic activity of CDs/MWCNTs nanocomposites, we used H_2O_2 as a probe molecule and examined the electrocatalytic properties of CDs/MWCNTs nanocomposites by cyclic voltammetry (CV) at a scan rate of 50 mV s^{-1}. Figure 3 shows the CVs obtained at GCE (a), CDs/GCE (b), MWCNTs/GCE (c), and CDs/MWCNTs-10/GCE (d) in 0.1 M pH 7.4 PBS in the absence (red line) and presence (black line) of 1.0 mM H_2O_2. Compared to the pure electrolyte, a negligible current response with onset potentials negative than 0.0 V occurs at GCE and CDs/GCE in the presence of 1.0 mM H_2O_2. An apparent peak at −0.2 V with onset potentials 0.0 V corresponding to the reduction of H_2O_2 was observed at MWCNTs/GCE (Fig. 3c). The increase of current indicates the significant electrochemical activity of MWCNTs to H_2O_2. For CDs/MWCNTs nanocomposites, a catalytic reduction current further increase, and the onset potentials for H_2O_2 reduction towards positive shift. However, it must be noted that the CDs/MWCNTs-10 showed the highest onset potential at +0.15 V and highest peak current for H_2O_2 reduction, and the reduction peak current per unit concentration of H_2O_2 at CDs/MWCNTs-10 is 5.0 times higher than that of MWCNTs/GCE based on background-subtracted data. These results strongly indicate that the CDs/MWCNTs/GCE shows a good electrocatalytic activity towards H_2O_2 reduction. The electrocatalytic activity of CDs/MWCNTs nanocomposites is significantly better than single CDs or MWCNTs. Furthermore, the CDs/MWCNTs-10 nanocomposites showed the highest electrocatalytic activity than CDs/MWCNTs-5 and CDs/MWCNTs-20 (see ESM Fig. S4). One possible cause is that fewer CDs introduced into the CNTs (CDs/MWCNTs-20) may produce fewer defects and active sites, resulting in lower

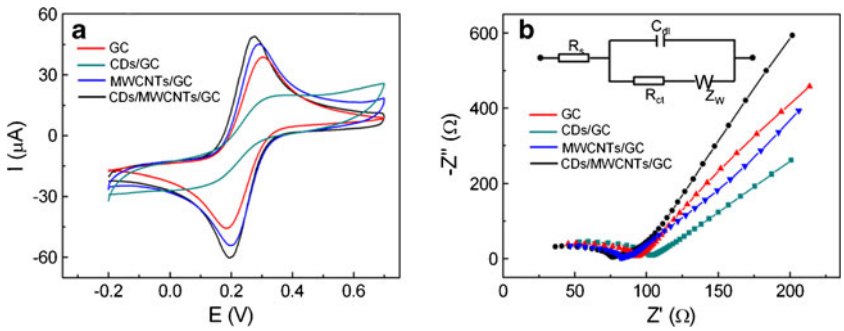

Fig. 2 Electrochemical characterization of the modified electrodes. **a** CVs and **b** Nyquist plots obtained at bare GC, CDs/GC, MWCNTs/GC, and CDs/MWCNTs-10/GC electrodes in 5.0 mM $[Fe(CN)_6]^{3-/4-}$/0.1 M KCl solution at a scan rate of 50 mV s^{-1}. Inset is the equivalent circuit

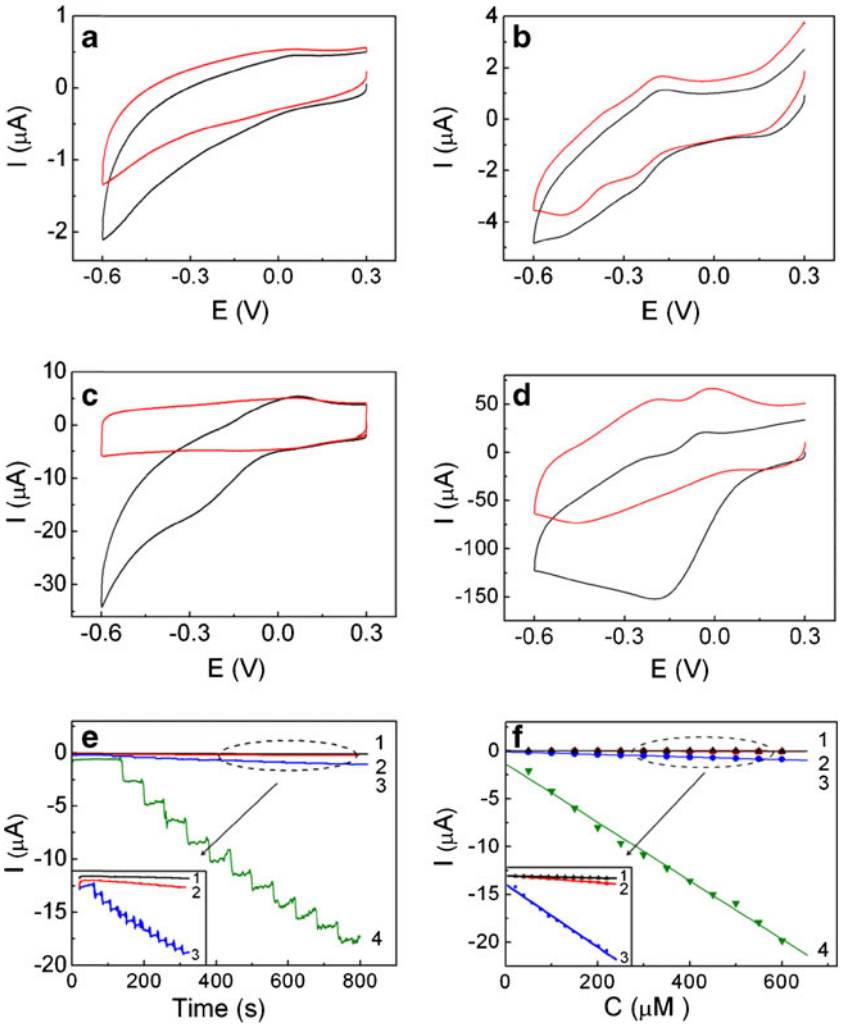

Fig. 3 Characterization of electrocatalytic activity. CVs recorded at **a** bare GC, **b** CDs/GC, **c** MWCNTs/GC, and **d** CDs/MWCNTs-10/GC electrodes in the absence (*red line*) and presence (*black line*) of 1.0 mM H_2O_2. Background electrolyte, 0.1 M PBS at pH 7.4. Scan rate: 50 mVs^{-1}. **e** Amperometric responses of the bare GC (1), CDs/GC (2), MWCNTs/GC (3), and CDs/MWCNTs-10/GC (4) electrodes with successive addition of 0.1 mM H_2O_2 into PBS (0.1 M, pH 7.4). **f** The related calibration curves

the electrocatalytic activity of CDs/MWCNTs nanocomposites. On the other hand, more CDs (CDs/MWCNTs-5), due to its poor electrical conductivity, effectively hindered the electron transfer between H_2O_2 and the electrode. Therefore, CDs/MWCNTs-10 nanocomposites are used to detect H_2O_2.

Furthermore, we compared the amperometric responses of the GCE, CDs/GCE, MWCNTs/GCE, and CDs/MWCNTs-10/GCE at a constant potential of −0.18 V to successive additions of 0.1 mM H_2O_2 in 0.1 M PBS as shown in Fig. 3e. When H_2O_2 is added into the buffer solution, the reduction current rises steeply and reaches a stable value, and the steady current increases with the increase of H_2O_2 concentration. Also, the response time of the sensor to achieve the steady-state current is <10, 10, 7, and 5 s for GCE, CDs/GCE, MWCNTs/GCE, and CDs/MWCNTs-10/GCE, respectively. It can be observed that the CDs/MWCNTs-10/GCE sensor exhibits faster response and larger reaction current to the change of H_2O_2 concentration. Figure 3f shows the calibration curves established by taking the steady-state current from Fig. 3e. The corresponding sensitivities at GCE, CDs/GCE, MWCNTs/GCE, and CDs/MWCNTs-10/GCE are calculated to be 0.041, 0.160, 1.34, and 39.0 μA/mM, respectively (the slope of the calibration plot). Obviously, the CDs/MWCNTs-10/GCE exhibits higher sensitivity compared with other electrodes. The enhanced electrocatalytic property of CDs/MWCNTs-10/GCE could be ascribed to the significant synergistic effects of the composites towards H_2O_2 reduction.

It has been reported that the defect-rich carbon nanotubes facilitate the formation of catalytic sites for the enhanced electrocatalytic activity. The defect-rich nature of the carbon nanotubes is evident from its high D-band/G-band ratio in Raman spectroscopy. As shown in Fig. 4, they both show two characteristic bands of CNTs. The D band at 1328 cm^{-1} is assigned to the defects and disordered graphite structures, and the G band at 1560 cm^{-1} originates from the graphite band corresponding to the movement in opposite directions of the C–C bonds in graphene sheets [26, 38]. Intensity ratio of defect band and graphite band (I_D/I_G) is proportional to the number of defect sites in the CNT sheets. The I_D/I_G values are 0.44 and 0.76 for MWCNTs and CDs/MWCNTs-10, respectively. An increase of

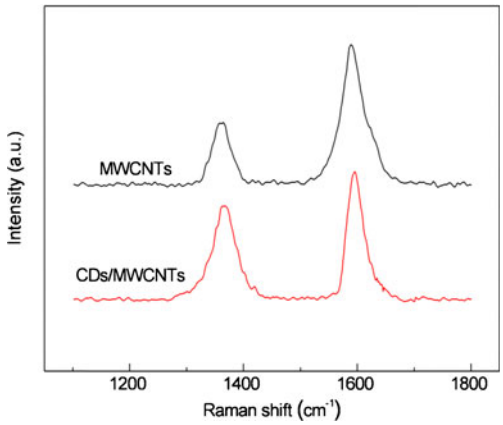

Fig. 4 Raman spectra of MWCNTs and CDs/MWCNTs-10

I_D/I_G ratios indicate that the presence of CDs on the MWCNTs introduced more structural defects on the surface of MWCNTs, which generally attributed to sp^2 carbons converted to sp^3 hybridization [39]. In this case, an increased defect density could presumably result in larger electrocatalytic activity.

In addition, previous studies had shown that the ability to provide lattice oxygen is also an important factor dictating the catalytic activity of catalyst [40]. Therefore, the X-ray photoelectron spectroscopy (XPS) was employed to evaluate the amount of lattice oxygen in carbon-based materials. Figure 5a shows the XPS survey spectra of CDs, MWCNTs, and CDs/MWCNTs-10 nanocomposites, revealing the only presence of carbon and oxygen atoms with no other impurities. The high-resolution O1s spectra were separated using the Gaussian–Lorentzian curve fitting method and deconvoluted into contributions from both lattice oxygen (LO) (≤532 eV) and adsorbed oxygen (AO) (≥533 eV) [41]. The LO/AO atomic ratio were evaluated to be 0.91, 0.66, and 2.28 for CDs (b), MWCNTs (c), and CDs/MWCNTs-10 (d), respectively, determined from the peak areas including the sensitivity factor. It should be noted that the introduction of CDs results in the increased proportion of LO in composites. Similar to previous study, a possible mechanism is that the withdrawing of electrons from surrounding carbon atoms by lattice oxygen can cause a carbon atom to become positively charge, which provides both the adsorption site and active catalytic site for H_2O_2 reduction [41]. That is to say, the enhancement of the electrocatalytic activity of CDs/MWCNTs-10 nanocomposites could be ascribed to high content of lattice oxygen. Therefore, increased LO/AO percentage in CDs/MWCNTs-10 composites could also cause an enhanced electrocatalytic activity.

Based on the above analysis and previous reports, the enhancement of the electrocatalytic activity of CDs/MWCNTs-10 nanocomposites could be ascribed to unique surface architecture. First, the MWCNTs as the conductive supports could improve the electron transfer from CDs/MWCNTs-10 surface to GC electrode. Second, the π–π conjugation between MWCNTs and CDs, as an electron transfer channel, offers an ultrafast

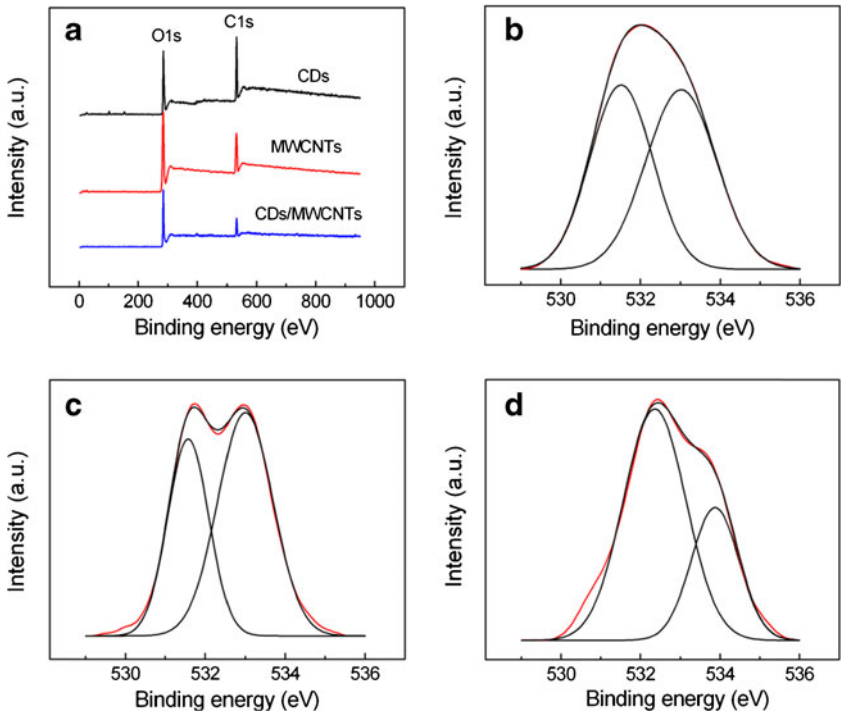

Fig. 5 **a** XPS spectra of CDs, MWCNTs and CDs/MWCNTs-10 nanocomposites. O1s spectra of **b** CDs, **c** MWCNTs, and **d** CDs/MWCNTs-10 naocomposites

charge transfer. Third, the defect-rich CNTs introduced by integrated CDs facilitate the formation of active sites for electron transfer to molecules. Additionally, the CDs/MWCNTs-10 nanocomposites have more lattice oxygen, which provide both the adsorption site and active catalytic site [42]. In a word, the combination of above factors brings an electrocatalytic synergy of CDs/MWCNTs-10 nanocomposites towards hydrogen peroxide reduction.

This excellent electrocatalytic performance of the CDs/MWCNTs-10 nanocomposites makes them promising electrochemical sensing materials for H_2O_2 detection. Amperometric responses of CDs/MWCNTs-10 nanocomposites to successive concentration changes of H_2O_2 were conducted at the potential of −0.18 V, and the corresponding current-time responses are shown in Fig. 6a. As shown, a well-defined amperometric response was observed upon each addition of H_2O_2, and the current response was a linear relationship with H_2O_2 concentration in the range of 3.5×10^{-6} to 3.0×10^{-4} M. The linear regression equation was expressed as follows: $I\ (\mu A) = -1.84e^{-7} - (0.039 \pm 0.00081)C\ (\mu M)$, with a correlation coefficient of 0.9993 (Fig. 6b), and the detection limit is estimated to be 0.25 μM at a signal/noise ratio of 3, which is lower than the most HRP enzyme [43, 44], noble metal nanomaterials [45], and carbon-based biosensors [46]. The analytical performance of the CDs/MWCNTs-10/GCE sensor for the detection of H_2O_2 and some other sensors are summarized in ESMTable S1.

Selectivity, reproducibility, and stability of the H_2O_2 biosensor

The influence of common interfering species on the response of sensor to 0.1 mM H_2O_2 was evaluated and presented in Fig. 6c. As can be seen, there was an obvious current response to the addition of 0.1 mM H_2O_2 at the first time, while no observable current response was detected to the additions of 0.2 mM ascorbic acid (AA), 0.2 mM uric acid (UA), 0.2 mM dopamine (DA), 0.2 mM acetaminophen (AP), 0.2 mM citric acid, and 0.2 mM glucose in the determination of H_2O_2, indicating that the CDs/MWCNTs-10/GCE shows a superior selectivity to H_2O_2 detection.

Based on the well electrochemical property, the CDs/MWCNTs-10 nanocomposites can be used as a new class of electrode material for electrochemical applications, so the tests of reproducibility and stability are very important. To evaluate the reproducibility of the proposed sensor, the six parallel measurements of CDs/MWCNTs-10/GCE to 1.0 mM of H_2O_2 were carried out independently. The relative standard deviation (RSD) was 4.43 %, which clearly indicated that the proposed sensor exhibited good reproducibility. The storage stability of the sensor was also monitored by recording the current response to 1.0 mM of H_2O_2 each day for 2 weeks. When the sensor was not in use, it was stored at 4 °C. As shown in Fig. 6d, the current response reduced slightly; however, 93 % of the original value remained after 14-day measurement,

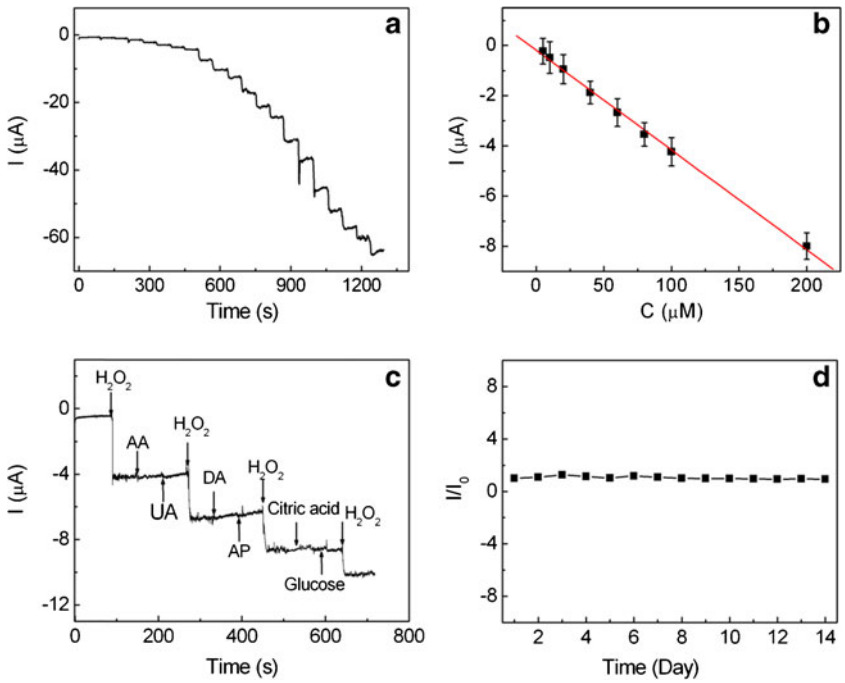

Fig. 6 Detection of H_2O_2. **a** Amperometric response of CDs/MWCNTs-10/GCE to successive additions of H_2O_2 at the potential of −0.18 V. **b** The corresponding calibration plots for CDs/MWCNTs-10/GCE. **c** Amperometric responses recorded at CDs/MWCNTs-10/GC electrode on the successive addition of 0.1 mM H_2O_2 followed by additions of 0.2 mM AA, 0.2 mM UA, 0.2 mM DA, 0.2 mM AP, 0.2 mM Citric acid, and 0.2 mM Glucose in PBS at pH 7.4. **d** Variation of CDs/MWCNTs-10/GCE response currents in the presence of 1.0 mM H_2O_2 in PBS at pH 7.4 versus storage time at 4 °C

suggesting the favorable stability of the sensor. Also, the effect of media pH on the H_2O_2 detection was investigated over the range of pH 5.0 to 10.0 (see ESM Fig. S5). The response peak current of the sensor had no great change over full range of pH, indicating excellent stability of the senor. The good stability of CDs/MWCNTs-10/GCE can be attributed to the chemical stability of conductive nanocomposites.

Detection of H_2O_2 in biological sample

To testify the feasibility of the CDs/MWCNTs-10/GCE in practical analysis, the recovery measurements were carried out to determine the H_2O_2 content in human serum samples and the analytical results were listed in ESM Table S2. The serum was collected and immediately analyzed according to the general procedure (see ESM Fig. S6). The recovered ratio was investigated, and the value was in the range of 97–101 %. The results indicate that the determination of H_2O_2 using CDs/MWCNTs-10/GCE is practicable and reliable.

The sensitive CDs/MWCNTs-10 probe was applied to perform real-time tracking of H_2O_2 secretion by live cells, which plays an important role in host defense against various microbes as well as tumors [47]. Before the detection, the HeLa cells were grown at 37 °C in 5 % CO_2 in 100 cm^2 flasks. The cells were collected after the growth to 90 %, and around 2×10^6 cells were dispersed in 5 mL of PBS (pH 7.4) for electrochemical measurement. To stimulate the cells to release more H_2O_2, we used CdTe QDs as the stimulus. It was reported that CdTe QDs as a toxic molecules, can induced cell death by generating reactive oxygen species (ROS), such as hydrogen peroxide and various hydroperoxide radicals [48]. Thus, upon the addition of 10 mM CdTe QDs, a significant current increase about 0.029 μA was observed (Fig. 7), that corresponding to 0.074 μM H_2O_2 per millimole CdTe QDs as calculated from the regression equation in Fig. 6b, which further decreases down to the level of background signal after addition of a H_2O_2 scavenger catalase. The control experiment without cells do not generate significant response towards the addition of equal amount of CdTe QDs (curve a). These results indicate that the increase of the cathodic current is indeed from the reduction of H_2O_2 released by live cells. These observations demonstrate that our proposed biosensor is sensitive and reliable probes for intracellular H_2O_2 detection, which will be very promising for further physiological and pathological investigations.

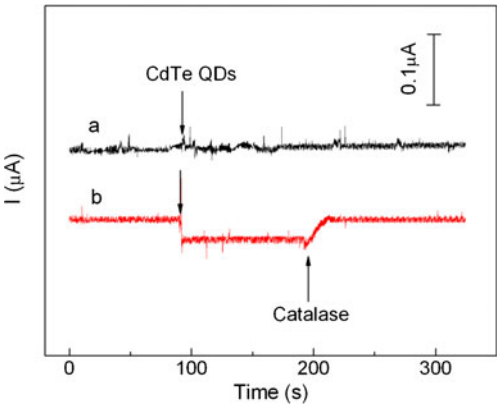

Fig. 7 Amperometric responses obtained at the CDs/MWCNTs-10/GCE in the absence (*black line*) and presence (*red line*) of HeLa cells in 25 mM glucose at the applied potential of −0.18 V vs Ag/AgCl with the addition of 10 mM CdTe QDs and 500 U mL^{-1} catalase

Conclusions

In summary, a novel H_2O_2 biosensor based on CDs/MWCNTs nanocomposites have been presented. The biosensor exhibited a good sensitivity, fast response, a broad linear range, a low detection limit with satisfactory stability, and selectivity for determination of H_2O_2. More importantly, the CDs/MWCNTs/GCE exhibited more enhanced electrocatalytic activities than CDs/GCE and MWCNTs/GCE towards the reduction of H_2O_2. The highly active CDs/MWCNTs nancomposites can be used for real-time detection of H_2O_2 released from HeLa cells. The high electrocatalytic activity of CDs/MWCNTs nanocomposites was attributed to the synergistic effect of the CDs and MWCNTs. Our present study provides a general strategy for the fabrication of carbon-based enzymeless H_2O_2 biosensors, which is important for biological and biomedical application.

Acknowledgments This work was financially supported by the National Science Foundation for Excellent Young Scholar of China (21322510), Science and Technology Innovation Foundation of Jilin Province for Talents Cultivation (Grants 20150519014JH), National Science Foundation for Young Scholar of China (21505130), and Youth Foundation of Jilin Province (20140520082JH).

Compliance with ethical standards

Conflict of interest The authors declare that they have no competing interests.

Human and animal rights and informed consent Informed consent was obtained from all individual participants included in the study. All procedures performed in studies involving human participants were in accordance with the ethical standards of the institutional and/or national research committee and with the 1964 Helsinki declaration and its later amendments or comparable ethical standards.

References

1. Ping J, Wu J, Fan K, Ying Y. An amperometric sensor based on prussian blue and poly(O-Phenylenediamine) modified glassy carbon electrode for the determination of hydrogen peroxide in beverages. Food Chem. 2011;126:2005–9.
2. Woo Y-A, Lim H-R, Kim H-J, Chung H. Determination of hydrogen peroxide concentration in antiseptic solutions using portable near-infrared system. J Pharm Biomed Anal. 2003;33:1049–57.
3. Lu X, Zhou J, Lu W, Liu Q, Li J. Carbon nanofiber-based composites for the construction of mediator-free biosensors. Biosens Bioelectron. 2008;23:1236–43.
4. Shu X, Chen Y, Yuan H, Gao S, Xiao D. H_2O_2 sensor based on the room-temperature phosphorescence of nano TiO_2/SiO_2 composite. Anal Chem. 2007;79:3695–702.
5. Baker SN, Baker GA. Luminescent carbon nanodots: emergent nanolights. Angew Chem Int Ed. 2010;49:6726–44.
6. Sies H. Biochemistry of oxidative stress. Angew Chem Int Ed Engl. 1986;25:1058–71.
7. Klassen NV, Marchington D, McGowan HCE. H_2O_2 determination by the I_3- method and by $KMnO_4$ titration. Anal Chem. 1994;66:2921–5.
8. Steinberg S. High-performance liquid chromatography method for determination of hydrogen peroxide in aqueous solution and application to simulated Martian soil and related materials. Environ Monit Assess. 2013;185:3749–57.
9. Matos RC, Coelho EO, Souza CF, Guedes FA, Matos MAC. Peroxidase immobilized on amberlite IRA-743 Resin for on-Line spectrophotometric detection of hydrogen peroxide in rainwater. Talanta. 2006;69:1208–14.
10. Wang T, Zhu H, Zhuo J, Zhu Z, Papakonstantinou P, Lubarsky G, et al. Biosensor based on ultrasmall MoS_2 nanoparticles for electrochemical detection of H_2O_2 released by cells at the nanomolar level. Anal Chem. 2013;85:10289–95.
11. Wang L, Zhu H, Song Y, Liu L, He Z, Wan L, et al. Architecture of poly(O-Phenylenediamine)–Ag nanoparticle composites for a hydrogen peroxide sensor. Electrochim Acta. 2012;60:314–20.
12. Bui M-PN, Pham X-H, Han KN, Li CA, Kim YS, Seong GH. Electrocatalytic reduction of hydrogen peroxide by silver particles patterned on single-walled carbon nanotubes. Sensors and Actuators B. 2010;150:436–41.
13. Wang L, Wang E. A novel hydrogen peroxide sensor based on horseradish peroxidase immobilized on colloidal Au modified ITO electrode. Electrochem Commun. 2004;6:225–9.
14. Prakash P, Agarwal R, Singh N, Chauhan RP, Agrawal VV, Biradar AM. Fabrication of enzyme based electrochemical H_2O_2 biosensor using TiO_2 as a matrix. Sens Lett. 2015;13:219–22.
15. Ernst A, Makowski O, Kowalewska B, Miecznikowski K, Kulesza PJ. Hybrid bioelectrocatalyst for hydrogen peroxide reduction: immobilization of enzyme within organic–inorganic film of structured prussian blue and PEDOT. Bioelectrochemistry. 2007;71:23–8.
16. Shoji E, Freund MS. Potentiometric sensors based on the inductive effect on the pk_a of poly(aniline): a nonenzymatic glucose sensor. J Am Chem Soc. 2001;123:3383–4.
17. Li X, Zhu Q, Tong S, Wang W, Song W. Self-assembled microstructure of carbon nanotubes for enzymeless glucose sensor. Sensors and Actuators B. 2009;136:444–50.
18. Xiao Y, Patolsky F, Katz E, Hainfeld JF, Willner I. "Plugging into enzymes": nanowiring of redox enzymes by a gold nanoparticle. Science. 2003;299:1877–81.
19. Zhang Y, Sun Y, Liu Z, Xu F, Cui K, Shi Y, et al. Au nanocages for highly sensitive and selective detection of H_2O_2. J Electroanal Chem. 2011;656:23–8.
20. Chen H, Zhang Z, Cai D, Zhang S, Zhang B, Tang J, et al. A hydrogen peroxide sensor based on Ag nanoparticles electrodeposited on natural nano-structure attapulgite modified glassy carbon electrode. Talanta. 2011;86:266–70.
21. Zhang L, Li H, Ni Y, Li J, Liao K, Zhao G. Porous cuprous oxide microcubes for non-enzymatic amperometric hydrogen peroxide and glucose sensing. Electrochem Commun. 2009;11:812–5.
22. Chang Q, Deng K, Zhu L, Jiang G, Yu C, Tang H. Determination of hydrogen peroxide with the aid of peroxidase-like Fe_3O_4 magnetic nanoparticles as the catalyst. Microchim Acta. 2009;165:299–305.
23. Zhang X, Liu D, Yu B, You T. A novel nonenzymatic hydrogen peroxide sensor based on electrospun nitrogen-doped carbon nanoparticles-embedded carbon nanofibers film. Sensors and Actuators B. 2016;224:103–9.
24. Lin W-J, Liao C-S, Jhang J-H, Tsai Y-C. Graphene modified basal and edge plane pyrolytic graphite electrodes for electrocatalytic oxidation of hydrogen peroxide and B-nicotinamide adenine dinucleotide. Electrochem Commun. 2009;11:2153–6.
25. Yang J, Liu D-J, Kariuki NN, Chen LX. Aligned carbon nanotubes with built-in FeN_4 active sites for electrocatalytic reduction of oxygen. Chem Commun. 2008; 329–31.
26. Zhou M, Guo J, Guo LP, Bai J. Electrochemical sensing platform based on the highly ordered mesoporous carbon-fullerene system. Anal Chem. 2008;80:4642–50.
27. Banks CE, Davies TJ, Wildgoose GG, Compton RG. Electrocatalysis at graphite and carbon nanotube modified electrodes: edge-plane sites and tube ends are the reactive sites. Chem Commun. 2005; 829–41.
28. Shao Y, Sui J, Yin G, Gao Y. Nitrogen-doped carbon nanostructures and their composites as catalytic materials for proton exchange membrane fuel cell. Appl Catal B. 2008;79:89–99.
29. Gong K, Du F, Xia Z, Durstock M, Dai L. Nitrogen-doped carbon nanotube arrays with high electrocatalytic activity for oxygen reduction. Science. 2009;323:760–4.
30. Shao Y, Zhang S, Engelhard MH, Li G, Shao G, Wang Y, et al. Nitrogen-doped graphene and its electrochemical applications. J Mater Chem. 2010;20:7491–6.
31. Shen J, Zhu Y, Yang X, Li C. Graphene quantum dots: emergent nanolights for bioimaging, sensors, catalysis and photovoltaic devices. Chem Commun. 2012;48:3686–99.
32. Li H, Kang Z, Liu Y, Lee S-T. Carbon nanodots: synthesis, properties and applications. J Mater Chem. 2012;22:24230–53.
33. Li Y, Zhao Y, Cheng H, Hu Y, Shi G, Dai L, et al. Nitrogen-doped graphene quantum dots with oxygen-rich functional groups. J Am Chem Soc. 2012;134:15–8.
34. Jahanbakhshi M, Habibi B. A novel and facile synthesis of carbon quantum dots via salep hydrothermal treatment as the silver nanoparticles support: application to electroanalytical determination of H2O2 in fetal bovine serum. Biosens Bioelectron. 2016;81:143–50.
35. Razmi H, Mohammad-Rezaei R. Graphene quantum dots as a new substrate for immobilization and direct electrochemistry of glucose oxidase: application to sensitive glucose determination. Biosens Bioelectron. 2013;41:498–504.
36. Kang SH, Choi SH, Kang MS, Kim JY, Kim HS, Hyeon T, et al. Nanorod-based dye-sensitized solar cells with improved charge collection efficiency. Adv Mater. 2008;20:54–8.
37. Teng X, Ma C, Ge C, Yan M, Yang J, Zhang Y, et al. Green synthesis of nitrogen-doped carbon dots from konjac flour with "Off-on" fluorescence by Fe^{3+} and L-lysine for bioimaging. J Mater Chem B. 2014;2:4631–9.
38. Jia N, Wang Z, Yang G, Shen H, Zhu L. Electrochemical properties of ordered mesoporous carbon and its electroanalytical application for selective determination of dopamine. Electrochem Commun. 2007;9:233–8.
39. Cañete-Rosales P, Ortega V, Álvarez-Lueje A, Bollo S, González M, Ansón A, et al. Influence of size and oxidative treatments of multi-walled carbon nanotubes on their electrocatalytic properties. Electrochim Acta. 2012;62:163–71.

40. Seo PW, Cho SP, Hong SH, Hong SC. The influence of lattice oxygen in titania on selective catalytic reduction in the low temperature region. Appl Catal A. 2010;380:21–7.
41. Zhou X, Tian Z, Li J, Ruan H, Ma Y, Yang Z, et al. Synergistically enhanced activity of graphene quantum dot/multi-walled carbon nanotube composites as metal-free catalysts for oxygen reduction reaction. Nanoscale. 2014;6:2603–7.
42. Sun H, Liu Z, Chen S, Quan X. The role of lattice oxygen on the activity and selectivity of the OMS-2 catalyst for the total oxidation of toluene. Chem Eng J. 2015;270:58–65.
43. Liu S-Q, Ju H-X. Renewable reagentless hydrogen peroxide sensor based on direct electron transfer of horseradish peroxidase immobilized on colloidal gold-modified electrode. Anal Biochem. 2002;307:110–6.
44. Zhang Y, Yuan R, Chai Y, Xiang Y, Hong C, Ran X. An amperometric hydrogen peroxide biosensor based on the immobilization of HRP on multi-walled carbon nanotubes/electro-copolymerized nano-Pt-poly(Neutral Red) composite membrane. Biochem Eng J. 2010;51:102–9.
45. Guo S, Wen D, Dong S, Wang E. Gold nanowire assembling architecture for H_2O_2 electrochemical sensor. Talanta. 2009;77:1510–7.
46. Liu M, Liu R, Chen W. Graphene wrapped Cu_2O nanocubes: non-enzymatic electrochemical sensors for the detection of glucose and hydrogen peroxide with enhanced stability. Biosens Bioelectron. 2013;45:206–12.
47. Dong S, Xi J, Wu Y, Liu H, Fu C, Liu H, et al. High loading MnO_2 nanowires on graphene paper: facile electrochemical synthesis and use as flexible electrode for tracking hydrogen peroxide secretion in live cells. Anal Chim Acta. 2015;853:200–6.
48. Tan SJ, Jana NR, Gao S, Patra PK, Ying JY. Surface-ligand-dependent cellular interaction, subcellular localization, and cytotoxicity of polymer-coated quantum dots. Chem Mater. 2010;22:2239–47.